

RSC Advances



This is an *Accepted Manuscript*, which has been through the Royal Society of Chemistry peer review process and has been accepted for publication.

Accepted Manuscripts are published online shortly after acceptance, before technical editing, formatting and proof reading. Using this free service, authors can make their results available to the community, in citable form, before we publish the edited article. This *Accepted Manuscript* will be replaced by the edited, formatted and paginated article as soon as this is available.

You can find more information about *Accepted Manuscripts* in the [Information for Authors](#).

Please note that technical editing may introduce minor changes to the text and/or graphics, which may alter content. The journal's standard [Terms & Conditions](#) and the [Ethical guidelines](#) still apply. In no event shall the Royal Society of Chemistry be held responsible for any errors or omissions in this *Accepted Manuscript* or any consequences arising from the use of any information it contains.

Rational design of Co-based redox mediators
for dye-sensitized solar cells by density functional theory

Zhu-Zhu Sun^{a,c}, Kui-Ming Zheng^{a,c}, Quan-Song Li^{a,c,*}, Ze-Sheng Li^{a,b,c,d,*}

^aKey Laboratory of Cluster Science of Ministry of Education, China

^bBeijing Key Laboratory for Chemical Power Source and Green Catalysis, China

^cSchool of Chemistry, Beijing Institute of Technology, Beijing 100081, China

^dThe Academy of Fundamental and Interdisciplinary Sciences, Harbin Institute of Technology,
Harbin 150080, China

Fax: +86 10 68911354; Tel: +86 10 68918670;

E-mail: Q.-S. Li: liquansong@bit.edu.cn, Z.-S. Li: zeshengli@bit.edu.cn

Keywords: Dye-sensitized solar cells, Redox mediators, Redox potential,
Reorganization energy, Density functional theory

Abstract

Density functional theory (DFT) calculations were carried out to explore the effects of alchemically modifying the polypyridine ligands and design efficient Co-based redox mediators for dye-sensitized solar cells (DSSCs). Our results showed that the redox properties of cobalt complexes can be well tuned by altering the number and position of nitrogen atoms on the ligand ring. Adding oxygen atoms on the ligand ring will evidently increase the redox potential, which might be unfavorable for the dye regeneration. The designed good redox mediators possess similar redox potential and reorganization energy to the current high-efficiency redox couples, thus are promising to be used in prospective DSSCs.

1 Introduction

Dye-sensitized solar cells (DSSCs) are considered as promising alternatives to conventional silicon-based solar cells due to their low material cost, good flexibility, and cost-effective technology.^{1, 2} As shown in Fig. 1, the basic DSSC structure consists of three fundamental components combined in a “sandwich” manner: a sensitized photoanode composed of a semiconductor nanoparticles (typically TiO₂) film on a transparent conductive oxide (TCO) glass covered with organic or metal-organic dyes, an electrolyte solution containing redox couple, solvent and additive in the middle, and a photocathode normally on platinized TCO glass. Note that there are six main electronic processes going on in DSSCs indicated by arrows in Fig. 1, where three steps (iii, iv, vi) are related with the redox mediator.

As one of the central components in DSSC, the redox mediator (or called redox couple) takes part in charge transfer and dye regeneration, which are key steps affecting the power conversion efficiency (PCE). The traditional redox mediator in DSSCs is I⁻/I₃⁻ redox couple, which ensures rapid dye regeneration by I⁻, slow recombination of photo injected electrons in TiO₂ with I₃⁻, and efficient positive charge transportation to the counter electrode.^{3,4} However, the I⁻/I₃⁻ redox couple has several disadvantages such as its corrosivity towards most high conductivity metals, the easy formation of polyiodides (I₅⁻, I₇⁻ and I₉⁻) that can absorb a large number of visible light, and its redox potential limiting the open voltage to about 0.8 V.^{5,6} In this respect, these drawbacks of I⁻/I₃⁻ redox couple hinder the efficiency improvement of DSSCs. Thereby a large number of I⁻/I₃⁻ free redox couples, including organic

compounds,⁷⁻¹² inorganic materials,¹³⁻¹⁵ and transition metal (Fe, Co, Ni, Cu) complexes,¹⁶⁻²⁰ have been synthesized and successfully applied in DSSCs. Among the metal complexes, the Co-based compounds are the most promising alternative redox couples because they have negligible absorption in the visible region of the solar spectrum and their redox properties can be regulated in a controlled manner by selecting suitable donor/acceptor substituents on the ligand.^{17, 18} The reported good Co-based redox couples ($[\text{Co}(\text{dbbip})_2]^{2+/3+}$, $[\text{Co}(\text{bpy})_3]^{2+/3+}$, $[\text{Co}(\text{dm-bpy})_3]^{2+/3+}$, $[\text{Co}(\text{dtb-bpy})_3]^{2+/3+}$, $[\text{Co}(\text{abpn})_2]^{2+/3+}$, $[\text{Co}(\text{phen})_3]^{2+/3+}$, $[\text{Co}(\text{Cl-phen})_3]^{2+/3+}$, $[\text{Co}(\text{NO}_2\text{-phen})_3]^{2+/3+}$, $[\text{Co}(\text{bpy-pz})_2]^{2+/3+}$, $[\text{Co}(\text{ttb-tpy})_2]^{2+/3+}$, et al) in conjunction with proper dyes have produced highly efficient DSSCs in recent years.¹⁶⁻²⁴ In 2011, the co-sensitization of dyes Y123 and YD2-o-C8 in combination with the $[\text{Co}(\text{bpy})_3]^{2+/3+}$ redox couple has achieved a PCE of 12.3%.²⁵ Recently, fabrication of DSSCs utilizing the porphyrin sensitizer SM315 and the $[\text{Co}(\text{bpy})_3]^{2+/3+}$ redox couple demonstrated panchromatic light harvesting without the use of co-sensitization, leading to a record 13% PCE at full sun illumination.²⁶

On the theoretical side, much less than the extensive studies on the sensitizing dyes and the photo-electrode materials,^{24, 27-39} very few attentions have been paid on the computational design of redox couples for DSSCs.^{40, 41} Coote and co-workers carried out high-level first principle calculations on the redox properties of a large number of nitroxides, and recommended some of them as efficient redox mediators for DSSCs.⁴⁰ They highlighted that an effective redox mediator must reversibly undergo one-electron oxidation and it must possess an oxidation potential in a range

of 0.60-0.85 V (vs. a standard hydrogen electrode in acetonitrile at 25 °C).⁴⁰ In the study of interfacial electron-transfer reactions from nanoparticle TiO₂ to redox couple [Co(t-Bu₂bpy)₃]^{2+/3+}, Ondersma and Hamann developed a useful model that can predict the efficiency of DSSCs as a function of the redox potential and the reorganization energy.⁴¹ The model indicates that to achieve over 20% efficiency in DSSCs is possible by using redox shuttles with more positive redox potentials and low reorganization energies.⁴¹ However, to our best knowledge, until now there is no systematic theoretical design of metal organic redox couples for DSSCs.

In this work, we have employed accurate computational methodologies to calculate the redox potential and reorganization energy of a series of Co complexes for screening good redox couples for high-efficiency DSSCs. The calculations were carried out in two steps. Firstly, we computed the redox potential of some classic Co complexes using various density functional theory (DFT) methods and compared the obtained values with the experimental data to select the best DFT method for further design. Next, using the validated method we designed several novel redox couples with suitable redox properties for solar cell applications.

2 Computational details

The Co-based redox couples are characterized by the redox potential and the reorganization energy. The redox potential E_{redox} relative to the normal hydrogen electrode (NHE) can be obtained by computing the free energy difference ΔG_{redox} between the Co(II) and Co(III) species: $-FE_{redox} = \Delta G_{redox}$, where $F = 23.06$ kcal.mol⁻¹.v⁻¹ is the Faraday constant. The ΔG_{redox} was calculated by $\Delta G_{redox} =$

$\Delta G_{vac} + \Delta\Delta G_{solv} - \Delta G_{NHE}$, where $\Delta G_{vac} = G_{vac}^{2+} - G_{vac}^{3+}$ is the gas-phase free energy difference; ΔG_{NHE} is a constant of -4.43 eV for the vacuum level with respect to NHE in water.⁴² It should be pointed out that the absolute potential of NHE is still a debated topic, with values ranging from 4.28 to 4.44 V.⁴³⁻⁴⁸ Hence, there may exist systematic errors in our computed redox potentials up to 0.15 V. G_{vac} is obtained by performing a single point calculation at the optimized geometry in vacuum, followed by frequency calculations in order to include the vibrational contribution to the total partition function. The free energy difference of solvation $\Delta\Delta G_{solv}$ is gotten by $\Delta\Delta G_{solv} = \Delta G_{solv}^{2+} - \Delta G_{solv}^{3+}$, where ΔG_{solv}^{2+} or ΔG_{solv}^{3+} is obtained by a single-point calculation in solution and a reference calculation in gas phase at the geometry optimized in solution. The reorganization energy was calculated as the difference between the single-point energy of the Co(II) complex at the geometry of the Co(III) complex and the ground-state energy of the Co(II) complex.

Geometry optimizations and vibrational frequency calculations were carried out in gas phase and in acetonitrile solution by using DFT methods. Solvation effects were included by means of conductor-like polarizable continuum model (C-PCM).⁴⁹
⁵⁰ We employed the UFF radii, which are explicitly optimized to reproduce the experimental solvation energy of a series of Co complexes.⁵¹ Open-shell molecules containing transition metals like the Co(II) complexes are notoriously difficult to get the correct electronic configuration, so the wavefunction stability was tested after optimization for the critical points. The counter-ions were not considered in this study based on the fact that the energy level shift between the ground state and the excited

state is less than 0.1 eV in previous assessment studies.⁵² The details about the employed DFT functionals, basis sets, and pseudo potential were explicitly explained in the following method calibration part.

All the calculations were performed on the Gaussian 09 programs.⁵³

3 Results and discussion

3.1 Method calibration

To find a suitable theoretical tool for further designing of new Co-based redox couples, a variety of levels of theory were tested on several classic Co complexes in Fig. 2. The obtained ΔG_{redox} together with the experimental values were given in Table 1.

Co(II) complexes, with a d^7 electronic configuration, can exist in a low spin (LS) doublet state or a high spin (HS) quartet state, where the two spin states may interconvert thermally.⁵⁴ Meanwhile, Co(III) complexes, having a d^6 electronic configuration, are generally in LS singlet state because the triplet state lies at much higher energy.⁵⁴ Therefore, we have considered the LS and HS state for Co(II) complexes and the LS state for Co(III) complexes in this section. An interesting issue about Co(II) complexes is which spin state (HS or LS) is more stable. From a ligand-field theoretical point of view, in a weak ligand field the HS state is the electronic ground state, while in a strong ligand field the ground state is the LS state.⁵⁴ Theoretical investigation and molar magnetic susceptibility research¹⁶ showed that many Co(II) complexes are more stable in HS state at room temperature. In the meantime, it's also found¹⁶ that there is a spin-crossover equilibrium between the

$^4\text{Co(II)}$ and the $^2\text{Co(II)}$ species, and the fast rate of HS to LS conversion created a high concentration of reactive LS species. As shown in Table 1, our calculations predict the HS state is lower in energy than the LS state for all the investigated Co(II) compounds except $[\text{Co}(\text{py}5\text{me}2)_2(\text{nmbi})]^{2+}$ at B3LYP/DZP level. This is consistent with the experimental observation of $[\text{Co}(\text{bpy})_3]^{2+}$ but in contrast with $[\text{Co}(\text{tpy})_2]^{2+}$ where the LS state is stabilized by the Jahn-Teller distortion of the axial ligands.⁵⁴ At B3LYP/LANL2DZ level, our results about $[\text{Co}(\text{bpy})_3]^{2+}$ are in line with previous theoretical study.¹⁶ In principle, both HS and LS Co(II) complexes could contribute to the dye regeneration reaction pathway because it is well known that dye generation in DSSCs consists of electron transfer from the $^2,4\text{Co(II)}$ complexes to the oxidized dye giving the Co(III) complexes.¹⁶

The calibration on the specific DFT functional and basis set proceeded in two steps. Firstly, we chose the LANL2DZ pseudo potential (which has been reported with good performance for transition metals)¹⁶ for cobalt and LANL2DZ basis set for other atoms, and tested several popular DFT functionals including B3LYP, CAM-B3LYP, MPW1PW91, and BHandHLYP. As shown in Table 1, compared with the experimental data, large mean errors of 0.66 eV and 1.59 eV were obtained for LS state and HS state with BHandHLYP, so this functional seems not suitable for these types of calculations and should be discarded. On the contrary, B3LYP shows the best performance with an average error of 0.02 eV for LS state and 0.24 eV for HS state with respect to the experimental data. At the same time both MPW1PW91 and CAM-B3LYP yield an average deviation of 0.11 eV for LS state and 0.4-0.5 eV for

HS state. Interestingly, the absolute differences between the MPW1PW91 results and B3LYP results are approximately 0.1 eV for LS state and 0.3 eV for HS state for all redox mediators investigated here. Secondly, we studied the effect of different basis sets. To achieve this goal, we performed calculations with the B3LYP method, LANL2DZ pseudo potential for Co, and three different basis sets including LANL2DZ, 6-31G** and DZP. Note that the DZP basis set defines the electron orbital for every atom specially, so there is no need to use any pseudo potential even for cobalt. The results in Table 1 disclosed that 6-31G** basis set overestimates the ΔG_{redox} values by 0.15 eV for LS state and 0.42 eV for HS state compared with the experimental values. Meanwhile, the DZP basis set provides similar results with the LANL2DZ basis set. As a result, the effect of basis set seems less important to the ΔG_{redox} values than that of the functional.

To conclude, the computational protocol clearly shows that the B3LYP functional together with the LANL2DZ basis set and pseudo potential is the best methodology on describing the redox potentials for cobalt complexes.

3.2 Designed redox couples based on cobalt complexes

The overall conversion efficiency (η) of DSSCs is determined by three factors: the open circuit potential (V_{OC}), the short-circuit current (J_{SC}), and the fill factor (FF).⁵⁵ All these three factors are related with the redox couple. The V_{OC} corresponds to the difference of the quasi-Fermi level of electrons in the nanocrystalline TiO_2 under illumination and the redox potential of the redox couple. The J_{SC} and FF are affected by the transport of redox-pair in the electrolyte and the electron transfer processes in

the dye regeneration by the redox couple and the reduction of the redox couple by the catalyst on the counter electrode.⁶ Therefore, an efficiency redox couple requires two key factors: (1) a proper redox potential which must guarantee a large enough open circuit potential and must be lower than the ground state oxidation potential of the dye to make sure the smooth progress of dye regeneration, and (2) a low reorganization energy which ensures a rapid electron transfer in the regeneration of the oxidized dye and the oxidized redox couple.⁴¹

Compared with bidentate ligands, tridentate ligands are expected to improve the stability of the cobalt complex significantly with the photovoltaic efficiency over 10%.²⁰ In addition, previous studies have revealed the changing trend of E_{redox} affected by substituent on the ligands: the introduction of electron-donor substituents on the ligands lowers the redox potential and the presence of electron acceptors results in higher E_{redox} .¹⁶⁻¹⁸ But it hasn't been clearly established how the ring structure of the ligand influences the physicochemical properties of the redox couple. As a result, in this section a set of new redox couples have been designed based on two classic tridentate cobalt complexes, $[Co(tpy)_2]^{2+/3+}$ and $[Co(bpy-pz)_2]^{2+/3+}$, by adjusting the ring structure of the ligand. At the same time, we summarized the influence of structural changes to the redox potential and reorganization energy. The structures of the designed redox mediators (Z1-Z12) together with three classic redox couples (C1-C3) are shown in Fig.3.

Since it is revealed in the method calibration part the high-spin isomers of Co(II) complexes are energetically favored, thereafter we mainly discuss the results of HS

state for Co(II) complexes except when otherwise stated. The selected key geometric parameters at B3LYP/LANL2DZ level of the designed redox couples (Z1-Z12) are depicted in Table 2, where the atomic labels (N1, N2, N3) are given in Fig. 3. Comparison of the N-Co-N angles and the Co-N bond lengths for cobaltous and trivalent cobalt complexes reveals that the major changes upon oxidation are the enlargement of the N-Co-N angles (N1-Co-N2 and N2-Co-N3) by 5-7 degrees, and the shortening of Co-N bond lengths (Co-N1, Co-N2 and Co-N3) by 0.2-0.3 Å. For Z3 and Z6, one nitrogen atom (N1) on the ring is replaced by an oxygen (O) atom, where the Co-O bond lengths are slightly shorter than those of Co-N and the O-Co-N angles are somewhat larger than those of N-Co-N. Nevertheless, the changes in Co-O bond lengths and Co-O-N angles due to oxidation are almost equivalent with the corresponding geometric parameters (Co-N angles and N-Co-N angles) in other redox couples without O in Table 2.

To assess the new designed redox couples, the two most important parameters for the evaluation of the redox properties, the redox potential (ΔG_{redox} or E_{redox}) and the reorganization energies (λ) of the designed redox couples Z1-Z12, three classic redox mediators C1-C3, and two efficient organic dyes Y123²⁰ and L0^{56, 57} are displayed in Table 3 and Fig. 4.

It is worth noting that Z1 has an almost equivalent E_{redox} for LS state and similar E_{redox} for HS state with C2 which yielded high power conversion efficiency over 10%.²⁰ Focusing on the structure of parazole (C2) and pyrimidine (Z1), we found that both of them have two nitrogen atoms, but parazole is a five-membered ring and

pyrimidine is a six-membered ring. It is clear that the redox potential is insensitive to the ring structure of the ligand, that is, in spite of five-membered ring or six-membered ring. More generally if there are equivalent N atoms in the ligands for two Co complexes, for example Z1/C2 and Z2/Z5, their redox potentials are almost equal. Interestingly, the ΔG_{redox} increases by 0.3-0.4 eV when one carbon atom on pyridine or pyrazole ring was replaced by one nitrogen atom, see C1/Z1/Z2 and Z4/C2/Z5. Adding nitrogen atoms on the outer ring of the ligand (from Z7 to Z8) will increase the redox potential as well, but the amplification is reduced by half than that on the inner ring. The position of N on the ring has negligible effects to the redox properties, as can be seen by the comparison of Z11 and Z12 where the middle ring is pyrimidine or pyrazine. When a nitrogen atom on the ring is replaced by an oxygen atom, for example C1 and Z3, the redox potential will shift to the higher potential direction by 0.87 V for LS state and 1.08 V for HS state. This kind of shift is more evident (1.27 V for LS state and 1.40 V for HS state) in case of five-membered ring, see Z4 and Z6. Note that the redox potentials of Z3 and Z6 are higher than the ground state oxidation potential of dyes L0 and Y123, which suggests the two oxygen-containing redox couples cannot regenerate these two oxidized dyes. Therefore, it should be caution for the experimentalists to introduce oxygen in the ligand to tune the redox potentials of Co-based redox mediators due to the large changing proportion.

In short, the redox potential is not sensitive to the size of the ring or the relative position (ortho/meta/para) of multiple nitrogen atoms, but subtle to the number of

nitrogen/oxygen atom on it.

Besides the redox potential, the inner-sphere reorganization energy (λ) is another important parameter for evaluating the redox mediators in DSSC,⁵⁸ because the reorganization energy can be used to estimate the kinetics of the regeneration process in the framework of Marcus theory.⁵⁹ In light of Marcus theory, small reorganization energy results in fast electron-transfer rate and thus favors high photovoltaic efficiency.⁴¹ Note that the reorganization energy is normally separated into internal and external components. The obtained internal reorganization energies for HS state of classic Co redox couples were 1.3-1.6 eV (see Table 3), which are in reasonable agreement with the experimental data around 2 eV⁶⁰⁻⁶³ if the external reorganization energy of about 0.7 eV^{62, 63} is taken into account. The reorganization energy in this work refers to the internal reorganization energy except when otherwise stated. General looking at the λ values of all species in Table 3, the LS reorganization energies are 0.7-1.0 eV smaller than the HS ones. In case of identical nitrogen numbers, for example C2 and Z1, the reorganization energy of redox couple with five-membered ring ligand (C2) is about 0.1 eV higher than that with six-membered ring ligand (Z1). This means the latter is likely to ensure a faster dye regeneration process. Note that moving the pyrimidine ring from the side (Z1) to the middle (Z11) of the three rings has negligible effect to both the redox potential and the reorganization energy. In addition, Z9 has the highest reorganization energy of 1.777 eV, which is much higher than those of the three classic redox couples C1, C2 and C3. This implies dye regeneration involving Z9 must be slower than employing other

redox couples in Table 3.

Following a rule that ideal candidates should have redox potentials close to the classic redox mediators C1-C3 and low reorganization energies, the designed redox couples are classified as good redox mediators and poor redox mediators in Fig. 4. The good candidates (Z1, Z4, Z7, Z11 and Z12) are expected to be good redox shuttles which can get a high V_{OC} without gearing down the regeneration of dye in DSSCs.

In addition, it is worth to mention that high-throughput computational materials design is an emerging area of materials science. High-throughput calculation, which automatically calculates and analyzes thousands of materials and thus can systematically search the optimal materials, becomes more and more popular and possibly represents the future of materials design.⁶⁵

4 Conclusion

This work has been focusing on the calculation of redox potential and reorganization energy for a set of cobalt complexes, with the aim of establishing a computational protocol for the prediction by computer simulations of the redox mediator for efficient applications in DSSCs. We discovered that among the different employed DFT methods the hybrid functional B3LYP with LANL2DZ basis set provides the most accurate results for cobalt based redox shuttles.

At the reliable B3LYP/LANL2DZ level, we theoretically designed a series of new cobalt based redox couples. Their redox potential and reorganization energy were tuned by changing the number of nitrogen and oxygen atoms on the ligand ring. The

further fine regulation can be made by the selection of positions of additional nitrogens. Adding oxygen atoms in the ligand will evidently raise the redox potential, which might be unfavorable for the dye regeneration. Finally, some novel compounds (Z1, Z4, Z7, Z11 and Z12) have been recommended as potential excellent redox mediators in the building of high-efficiency DSSCs.

Acknowledgements

This work is financially supported by the Major State Basic Research Development Programs of China (2011CBA00701, 2012CB721003), the National Natural Science Foundation of China (21303007), the Specialized Research Fund for the Doctoral Program of Higher Education (20131101120053), the Excellent Young Scholars Research Fund of Beijing Institute of Technology (2013YR1917), the Basic Research Fund of Beijing Institute of Technology (20121942011, 20131942008), and Beijing Key Laboratory for Chemical Power Source and Green Catalysis (2013CX02031). This work is also supported by the opening project of State Key Laboratory of Science and Technology (Beijing Institute of Technology). The opening project number is XXXXXXXXX. ZDKT12-03.

Supplementary data

Cartesian coordinates of the optimized structures for classic and designed redox mediators in acetonitrile and in vacuum at B3LYP/LANL2DZ level.

References

- 1 A. Hagfeldt, G. Boschloo, L. C. Sun, L. Kloo and H. Pettersson, *Chem. Rev.*, 2010, **110**, 6595.
- 2 B. Oregan and M. Grätzel, *Nature*, 1991, **353**, 737.
- 3 R. Jono, M. Sumita, Y. Tateyama and K. Yamashita, *J. Phys. Chem. Lett.*, 2012, **3**, 3581.
- 4 J. G. Rowley, B. H. Farnum, S. Ardo and G. J. Meyer, *J. Phys. Chem. Lett.*, 2010, **1**, 3132.
- 5 T. W. Hamann, *Dalton. Trans.*, 2012, **41**, 3111.
- 6 J. Y. Cong, X. C. Yang, L. Kloo and L. C. Sun, *Energy Environ. Sci.*, 2012, **5**, 9180.
- 7 W. Cho, D. Song, Y. G. Lee, H. Chae, Y. R. Kim, Y. B. Pyun, S. Nagarajan, P. Sudhagar and Y. S. Kang, *J. Mater. Chem. A*, 2013, **1**, 233.
- 8 F. Kato, A. Kikuchi, T. Okuyama, K. Oyaizu and H. Nishide, *Angew. Chem. Int. Ed.*, 2012, **51**, 10177.
- 9 D. M. Li, H. Li, Y. H. Luo, K. X. Li, Q. B. Meng, M. Armand and L. Q. Chen, *Adv. Funct. Mater.*, 2010, **20**, 3358.
- 10 H. N. Tian, Z. Yu, A. Hagfeldt, L. Kloo and L. Sun, *J. Am. Chem. Soc.*, 2011, **133**, 9413.
- 11 M. K. Wang, N. Chamberland, L. Breau, J. E. Moser, R. Humphry-Baker, B. Marsan, S. M. Zakeeruddin and M. Grätzel, *Nat. Chem.*, 2010, **2**, 385.
- 12 Z. Zhang, P. Chen, T. N. Murakami, S. M. Zakeeruddin and M. Grätzel, *Adv. Funct. Mater.*, 2008, **18**, 341.
- 13 C. Teng, X. C. Yang, C. Z. Yuan, C. Y. Li, R. K. Chen, H. N. Tian, S. F. Li, A. Hagfeldt and L. C. Sun, *Org. Lett.*, 2009, **11**, 5542.
- 14 P. Wang, S. M. Zakeeruddin, J. E. Moser, R. Humphry-Baker and M. Grätzel, *J. Am. Chem. Soc.*, 2004, **126**, 7164.
- 15 Z. S. Wang, K. Sayama and H. Sugihara, *J. Phys. Chem. B*, 2005, **109**, 22449.
- 16 E. Mosconi, J. H. Yum, F. Kessler, C. J. G. Garcia, C. Zuccaccia, A. Cinti, M. K. Nazeeruddin, M. Grätzel and F. De Angelis, *J. Am. Chem. Soc.*, 2012, **134**, 19438.
- 17 H. Nusbaumer, S. M. Zakeeruddin, J. E. Moser and M. Grätzel, *Chem.-Eur. J.*, 2003, **9**, 3756.
- 18 S. A. Sapp, C. M. Elliott, C. Contado, S. Caramori and C. A. Bignozzi, *J. Am. Chem. Soc.*, 2002, **124**, 11215.
- 19 Y. L. Xie and T. W. Hamann, *J. Phys. Chem. Lett.*, 2013, **4**, 328.
- 20 J. H. Yum, E. Baranoff, F. Kessler, T. Moehl, S. Ahmad, T. Bessho, A. Marchioro, E. Ghadiri, J. E. Moser, C. Y. Yi, M. K. Nazeeruddin and M. Grätzel, *Nat. Commun.*, 2012, **3**, 631.
- 21 K. Ben Aribia, T. Moehl, S. M. Zakeeruddin and M. Grätzel, *Chem. Sci.*, 2013, **4**, 454.
- 22 S. M. Feldt, E. A. Gibson, E. Gabrielsson, L. Sun, G. Boschloo and A. Hagfeldt, *J. Am. Chem. Soc.*, 2010, **132**, 16714.
- 23 M. K. Kashif, J. C. Axelson, N. W. Duffy, C. M. Forsyth, C. J. Chang, J. R. Long, L. Spiccia and U. Bach, *J. Am. Chem. Soc.*, 2012, **134**, 16646.
- 24 M. K. Kashif, M. Nippe, N. W. Duffy, C. M. Forsyth, C. J. Chang, J. R. Long, L. Spiccia and U. Bach, *Angew. Chem. Int. Ed.*, 2013, **52**, 5527.
- 25 A. Yella, H. W. Lee, H. N. Tsao, C. Y. Yi, A. K. Chandiran, M. K. Nazeeruddin, E. W. G. Diau, C. Y. Yeh, S. M. Zakeeruddin and M. Grätzel, *Science*, 2011, **334**, 629.
- 26 S. Mathew, A. Yella, P. Gao, R. Humphry-Baker, B. F. E. Curchod, N. Ashari-Astani, I. Tavernelli, U. Rothlisberger, M. K. Nazeeruddin and M. Grätzel, *Nat. Chem.*, 2014, **6**, 242.
- 27 S. Ahmad, J. H. Yum, H. J. Butt, M. K. Nazeeruddin and M. Grätzel, *Chemphyschem*, 2010, **11**,

- 2814.
- 28 M. Al-Mamun, J. Y. Kim, Y. E. Sung, J. J. Lee and S. R. Kim, *Chem. Phys. Lett.*, 2013, **561**, 115.
- 29 J. H. Luo, Q. S. Li, L. N. Yang, Z. Z. Sun and Z. S. Li, *Rsc. Adv.*, 2014, **4**, 20200.
- 30 S. L. Chen, L. N. Yang and Z. S. Li, *J. Power Sources*, 2013, **223**, 86.
- 31 L. N. Yang, Z. Z. Sun, S. L. Chen and Z. S. Li, *Chemphyschem*, 2014, **15**, 458.
- 32 Q. Liu, Q. S. Li, G. Q. Lv, J. H. Luo, L. N. Yang, S. L. Chen and Z. S. Li, *Theor. Chem. Acc.*, 2013, **133**, 1437.
- 33 J. W. Li, X. Chen, N. Ai, J. M. Hao, Q. Chen, S. Strauf and Y. Shi, *Chem. Phys. Lett.*, 2011, **514**, 141.
- 34 J. Zhang, L. Yang, M. Zhang and P. Wang, *Rsc. Adv.*, 2013, **3**, 6030.
- 35 M. Nasr-Esfahani, M. Zendehtdel, N. Yaghoobi Nia, B. Jafari and M. Khosravi Babadi, *Rsc. Adv.*, 2014, **4**, 15961.
- 36 V. K. Singh, R. K. Kanaparthi and L. Giribabu, *Rsc. Adv.*, 2014, **4**, 6970.
- 37 J. M. Ball, N. K. S. Davis, J. D. Wilkinson, J. Kirkpatrick, J. Teuscher, R. Gunning, H. L. Anderson and H. J. Snaith, *Rsc. Adv.*, 2012, **2**, 6846.
- 38 P. S. Reeta, L. Giribabu, S. Senthilarasu, M.-H. Hsu, D. K. Kumar, H. M. Upadhyaya, N. Robertson and T. Hewat, *Rsc. Adv.*, 2014, **4**, 14165.
- 39 H. Li, Y. Li and M. Chen, *Rsc. Adv.*, 2013, **3**, 12133.
- 40 G. Gryn'ova, J. M. Barakat, J. P. Blinco, S. E. Bottle and M. L. Coote, *Chem.-Eur. J.*, 2012, **18**, 7582.
- 41 J. W. Ondersma and T. W. Hamann, *Coord. Chem. Rev.*, 2013, **257**, 1533.
- 42 H. Reiss and A. Heller, *J. Phys. Chem.*, 1985, **89**, 4207.
- 43 S. Trasatti, *Pure Appl. Chem.*, 1986, **58**, 955.
- 44 C. P. Kelly, C. J. Cramer and D. G. Truhlar, *J. Phys. Chem. B*, 2006, **110**, 16066.
- 45 W. R. Fawcett, *Langmuir*, 2008, **24**, 9868.
- 46 R. L. Lord, F. A. Schultz and M.-H. Baik, *J. Am. Chem. Soc.*, 2009, **131**, 6189.
- 47 A. A. Isse and A. Gennaro, *J. Phys. Chem. B*, 2010, **114**, 7894.
- 48 T. F. Hughes and R. A. Friesner, *J. Chem. Theory Comput.*, 2012, **8**, 442.
- 49 V. Barone and M. Cossi, *J. Phys. Chem. A*, 1998, **102**, 1995.
- 50 M. Cossi, N. Rega, G. Scalmani and V. Barone, *J. Comput. Chem.*, 2003, **24**, 669.
- 51 V. Barone, M. Cossi and J. Tomasi, *J. Chem. Phys.*, 1997, **107**, 3210.
- 52 M. K. Nazeeruddin, F. De Angelis, S. Fantacci, A. Selloni, G. Viscardi, P. Liska, S. Ito, T. Bessho and M. Grätzel, *J. Am. Chem. Soc.*, 2005, **127**, 16835.
- 53 M. J. T. Frisch, G. W.; Schlegel, H. B.; Scuseria, G. E.; Robb, M. A.; Cheeseman, J. R.; Scalmani, G.; Barone, V.; Mennucci, B.; Petersson, G. A.; Nakatsuji, H.; Caricato, M.; Li, X.; Hratchian, H. P.; Izmaylov, A. F.; Bloino, J.; Zheng, G.; Sonnenberg, J. L.; Hada, M.; Ehara, M.; Toyota, K.; Fukuda, R.; Hasegawa, J.; Ishida, M.; Nakajima, T.; Honda, Y.; Kitao, O.; Nakai, H.; Vreven, T.; Montgomery, J. A., Jr.; Peralta, J. E.; Ogliaro, F.; Bearpark, M.; Heyd, J. J.; Brothers, E.; Kudin, K. N.; Staroverov, V. N.; Kobayashi, R.; Normand, J.; Raghavachari, K.; Rendell, A.; Burant, J. C.; Iyengar, S. S.; Tomasi, J.; Cossi, M.; Rega, N.; Millam, N. J.; Klene, M.; Knox, J. E.; Cross, J. B.; Bakken, V.; Adamo, C.; Jaramillo, J.; Gomperts, R.; Stratmann, R. E.; Yazyev, O.; Austin, A. J.; Cammi, R.; Pomelli, C.; Ochterski, J. W.; Martin, R. L.; Morokuma, K.; Zakrzewski, V. G.; Voth, G. A.; Salvador, P.; Dannenberg, J. J.; Dapprich, S.; Daniels, A. D.; Farkas, Ö.; Foresman, J. B.; Ortiz, J. V.; Cioslowski, J.; Fox, D. J., *Gaussian 09, Revision A.01*, Gaussian, Inc., Wallingford CT, 2009.

- 54 I. Krivokapic, M. Zerara, M. L. Daku, A. Vargas, C. Enachescu, C. Ambrus, P. Tregenna-Piggott, N. Amstutz, E. Krausz and A. Hauser, *Coord. Chem. Rev.*, 2007, **251**, 364.
- 55 M. Grätzel, *Acc. Chem. Res.*, 2009, **42**, 1788.
- 56 T. Kitamura, M. Ikeda, K. Shigaki, T. Inoue, N. A. Anderson, X. Ai, T. Q. Lian and S. Yanagida, *Chem. Mater.*, 2004, **16**, 1806.
- 57 M. Pastore, S. Fantacci and F. De Angelis, *J. Phys. Chem. C*, 2010, **114**, 22742.
- 58 M. D. Newton, *Coord. Chem. Rev.*, 2003, **238**, 167.
- 59 R. A. Marcus and N. Sutin, *Biochim. Biophys. Acta.*, 1985, **811**, 265.
- 60 J. F. Endicott, B. Durham and K. Kumar, *Inorg. Chem.*, 1982, **21**, 2437.
- 61 A. Yoshimura, K. Nozaki, N. Ikeda and T. Ohno, *J. Phys. Chem.*, 1996, **100**, 1630.
- 62 G. A. Tsirlina, Y. I. Kharkats, R. R. Nazmutdinov and O. A. Petrii, *J. Electroanal. Chem.*, 1998, **450**, 63.
- 63 A. Yoshimura, M. J. Uddin, N. Amasaki and T. Ohno, *J. Phys. Chem. A*, 2001, **105**, 10846.
- 64 M. K. Wang, C. Grätzel, S. M. Zakeeruddin and M. Grätzel, *Energy Environ. Sci.*, 2012, **5**, 9394.
- 65 S. Curtarolo, G. L. W. Hart, M. B. Nardelli, N. Mingo, S. Sanvito and O. Levy, *Nat. Mater.*, 2013, **12**, 191.

Figure legends

Fig. 1 Schematic description of the constituent materials in DSSCs and the main electronic transfer processes taking place inside. Solid arrows indicate the positive processes and the dotted arrows indicate the deleterious processes.

Fig. 2 Molecular structure of classic Co-based redox mediators investigated in this work.

Fig. 3 Molecular structure of the classic (C1-C3) and designed (Z1-Z12) Co-based redox couples. C1: $\text{Co}(\text{tpy})_2$; C2 : $\text{Co}(\text{bpy-pz})_2$; C3: $\text{Co}(\text{bpy})_3$.

Fig. 4 The redox potential vs. reorganization energy map for the classic (C1-C3) and designed (Z1-Z12) redox couples. The Co(II) complexes are in HS state. For comparison, the redox potentials of classic dyes (L0 and Y123) are also displayed in dotted horizontal line. The two dotted vertical lines indicate the reorganization energies of C2 and C3, respectively.

Table 1

Calculated ΔG_{redox} (in eV) of for the investigated classic cobalt based redox mediators. Both low-spin (LS) state and high-spin (HS) state of Co(II) complexes are considered. For comparison the corresponding experimental data and mean unsigned errors with respect to the experimental data are also provided.

	B3LYP/ 6-31G**		B3LYP/ DZP		B3LYP/ LANL2DZ		CAM-B3LYP/ LANL2DZ		MPW1PW91/ LANL2DZ		BHand3LYP/ LANL2DZ		EXP
	LS	HS	LS	HS	LS	HS	LS	HS	LS	HS	LS	HS	
[Co(tpy) ₂] ^{2+/3+}	-5.25	-5.40	-5.08	-5.24	-5.05	-5.13	-5.12	-5.37	-5.15	-5.44	-5.69	-6.56	-4.93 ^a
[Co(bpy) ₃] ^{2+/3+}	-5.19	-5.53	-5.03	-5.29	-5.00	-5.27	-5.10	-5.42	-5.10	-5.57	-5.66	-6.63	-5.00 ^a
[Co(dbpip) ₂] ^{2+/3+}	-5.06	-5.45	-5.08	-5.25	-5.01	-5.15	-5.04	-5.30	-5.10	-5.46	-5.46	-6.43	-5.03 ^a
[Co(phen) ₂] ^{2+/3+}	-5.24	-5.42	-5.08	-5.35	-5.06	-5.36	-5.09	-5.51	-5.17	-5.67	-5.74	-6.71	-5.06 ^a
[Co(py5me2) ₂ (nmbi)] ^{2+/3+}	-5.33	-5.73	-5.46	-5.43	-5.24	-5.55	-5.37	-5.72	-5.36	-5.86	-5.91	-6.87	-5.29 ^b
[Co(bpy-pz) ₂] ^{2+/3+}	-5.48	-5.52	-5.31	-5.54	-5.31	-5.50	-5.58	-5.96	-5.41	-5.80	-6.03	-6.88	-5.30 ^a
[Co(py5me2) ₂ (tbp)] ^{2+/3+}	-5.46	-5.75	-5.27	-5.50	-5.33	-5.60	-5.46	-5.60	-5.45	-5.90	-6.01	-6.97	-5.34 ^b
[Co(py-pz) ₃] ^{2+/3+}	-5.54	-5.90	-5.37	-5.66	-5.38	-5.69	-5.46	-5.81	-5.48	-5.98	-6.11	-6.98	-5.40 ^c
Mean error	0.15	0.42	0.04	0.24	0.02	0.24	0.11	0.42	0.11	0.54	0.66	1.59	

^a References ⁶ and ⁶⁴.

^b References ²³.

^c References ³.

Table 2

Bond lengths and angles of the classic and designed redox couples (Co(II) complexes in HS state). The atomic labels (N1, N2, N3) are given in Fig. 3.

Compounds	Bond Length(Å)			Bond Angle(°)	
	Co-N1 ^a	Co-N2	Co-N3	N1-Co-N2	N2-Co-N3
[C1] ^{2+/3+}	2.17 / 1.98	2.08 / 1.89	2.20 / 1.98	76.6 / 82.5	76.5 / 82.5
[C2] ^{2+/3+}	2.15 / 1.96	2.09 / 1.89	2.20 / 1.96	76.5 / 82.6	75.5 / 81.7
[Z1] ^{2+/3+}	2.19 / 1.97	2.08 / 1.89	2.18 / 1.98	76.7 / 82.6	76.2 / 82.2
[Z2] ^{2+/3+}	2.18 / 1.97	2.08 / 1.89	2.21 / 1.99	76.9 / 82.4	76.1 / 82.1
[Z3] ^{2+/3+}	2.12 / 1.93	2.06 / 1.89	2.23 / 2.01	78.5 / 83.7	74.7 / 80.8
[Z4] ^{2+/3+}	2.17 / 1.97	2.09 / 1.90	2.18 / 1.94	76.4 / 82.6	77.4 / 83.1
[Z5] ^{2+/3+}	2.15 / 1.96	2.10 / 1.89	2.23 / 1.97	76.5 / 82.8	75.1 / 81.5
[Z6] ^{2+/3+}	2.11 / 1.92	2.06 / 1.90	2.30 / 2.02	78.6 / 83.5	74.7 / 80.8
[Z7] ^{2+/3}	2.18 / 1.97	2.09 / 1.90	2.19 / 1.96	76.0 / 82.2	77.3 / 82.3
[Z8] ^{2+/3+}	2.17 / 1.97	2.11 / 1.90	2.21 / 1.98	75.7 / 82.3	76.3 / 81.9
[Z9] ^{2+/3+}	2.17 / 1.98	2.07 / 1.89	2.17 / 1.98	77.0 / 82.3	77.0 / 82.3
[Z10] ^{2+/3+}	2.19 / 1.99	2.07 / 1.88	2.23 / 1.98	75.7 / 82.0	76.2 / 81.7
[Z11] ^{2+/3+}	2.18 / 1.98	2.07 / 1.86	2.22 / 1.99	75.9 / 82.0	76.4 / 82.3
[Z12] ^{2+/3+}	2.18 / 1.98	2.07 / 1.88	2.20 / 1.98	76.2 / 82.2	76.2 / 82.2

^a Co-O distance instead of Co-N1 distance for [Z3]^{2+/3+} and [Z6]^{2+/3+}.

Table 3

Calculated ΔG_{redox} , E_{redox} (vs NHE), and inner-sphere reorganization energy λ_{in} for the classic and new redox couples. Both low-spin (LS) state and high-spin (HS) state of Co(II) complexes are considered.

Compound	ΔG_{redox} (eV)		E_{redox} (V)			λ^{LS} (eV)	λ^{HS} (eV)
	LS	HS	LS	HS	EXP		
[C1] ^{2+/3+}	-5.05	-5.13	0.62	0.70	0.50 ^a	0.525	1.536
[C2] ^{2+/3+}	-5.31	-5.50	0.88	1.07	0.86 ^a	0.603	1.590
[C3] ^{2+/3+}	-5.00	-5.27	0.57	0.84	0.57 ^a	0.613	1.323
[Z1] ^{2+/3+}	-5.31	-5.42	0.88	0.99	--	0.524	1.539
[Z2] ^{2+/3+}	-5.58	-5.75	1.15	1.32	--	0.532	1.559
[Z3] ^{2+/3+}	-5.92	-6.21	1.49	1.78	--	0.564	1.391
[Z4] ^{2+/3+}	-4.91	-5.08	0.48	0.65	--	0.616	1.607
[Z5] ^{2+/3+}	-5.59	-5.78	1.16	1.35	--	0.593	1.574
[Z6] ^{2+/3+}	-6.18	-6.48	1.75	2.05	--	0.589	1.425
[Z7] ^{2+/3+}	-5.11	-5.39	0.68	0.97	--	0.626	1.565
[Z8] ^{2+/3+}	-5.37	-5.62	0.94	1.20	--	0.590	1.345
[Z9] ^{2+/3+}	-5.59	-5.73	1.16	1.30	--	0.523	1.777
[Z10] ^{2+/3+}	-5.68	-5.92	1.49	1.73	--	0.542	1.569
[Z11] ^{2+/3+}	-5.37	-5.47	0.94	1.04	--	0.525	1.539
[Z12] ^{2+/3+}	-5.39	-5.32	0.96	0.89	--	0.521	1.466
L0	--	--	--	--	1.38 ^b	--	--
Y123	--	--	--	--	1.09 ^c	--	--

^a References⁶ and ⁶⁴.

^b References⁵⁷.

^c References²⁰.

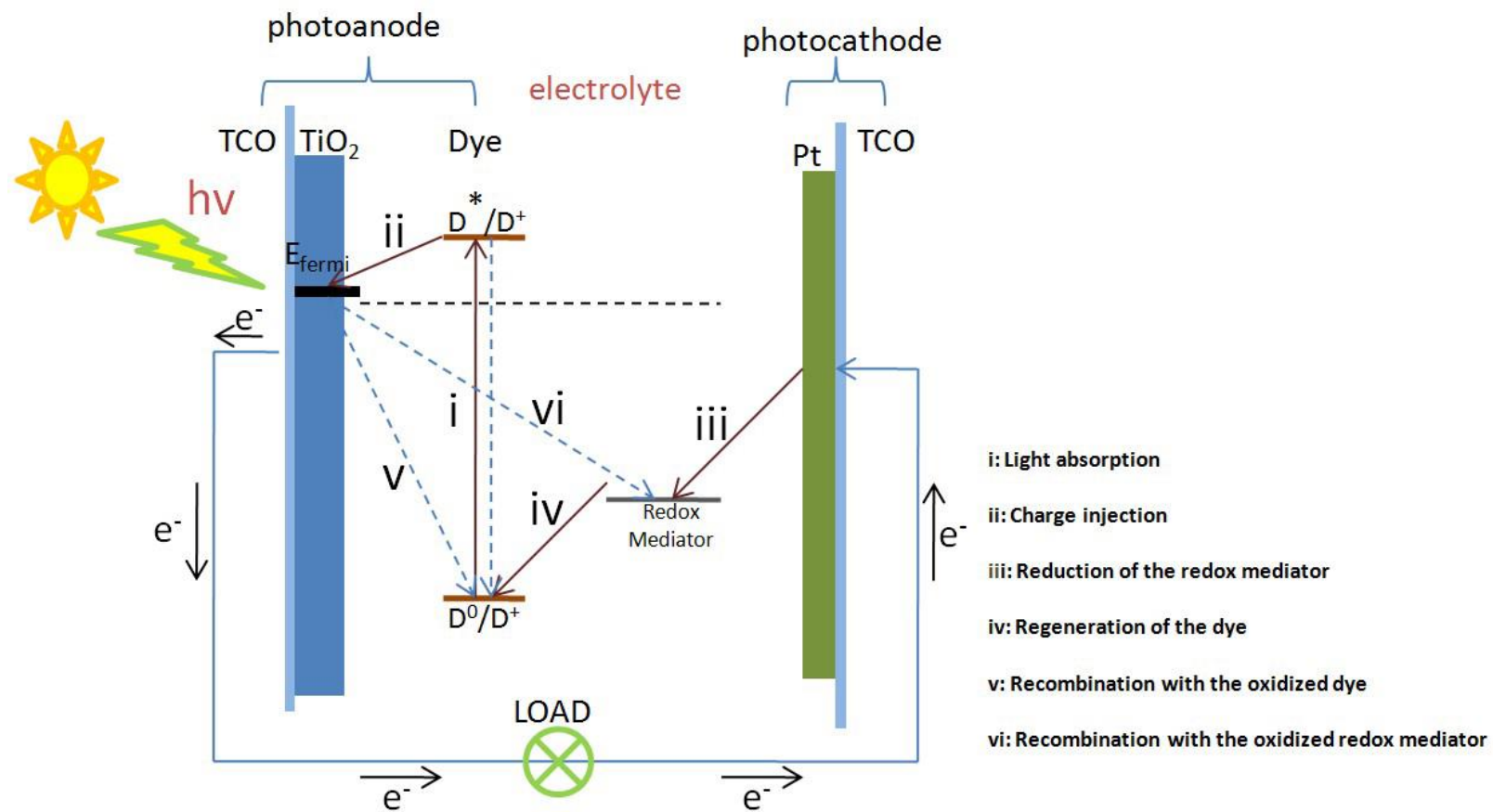


Fig. 1

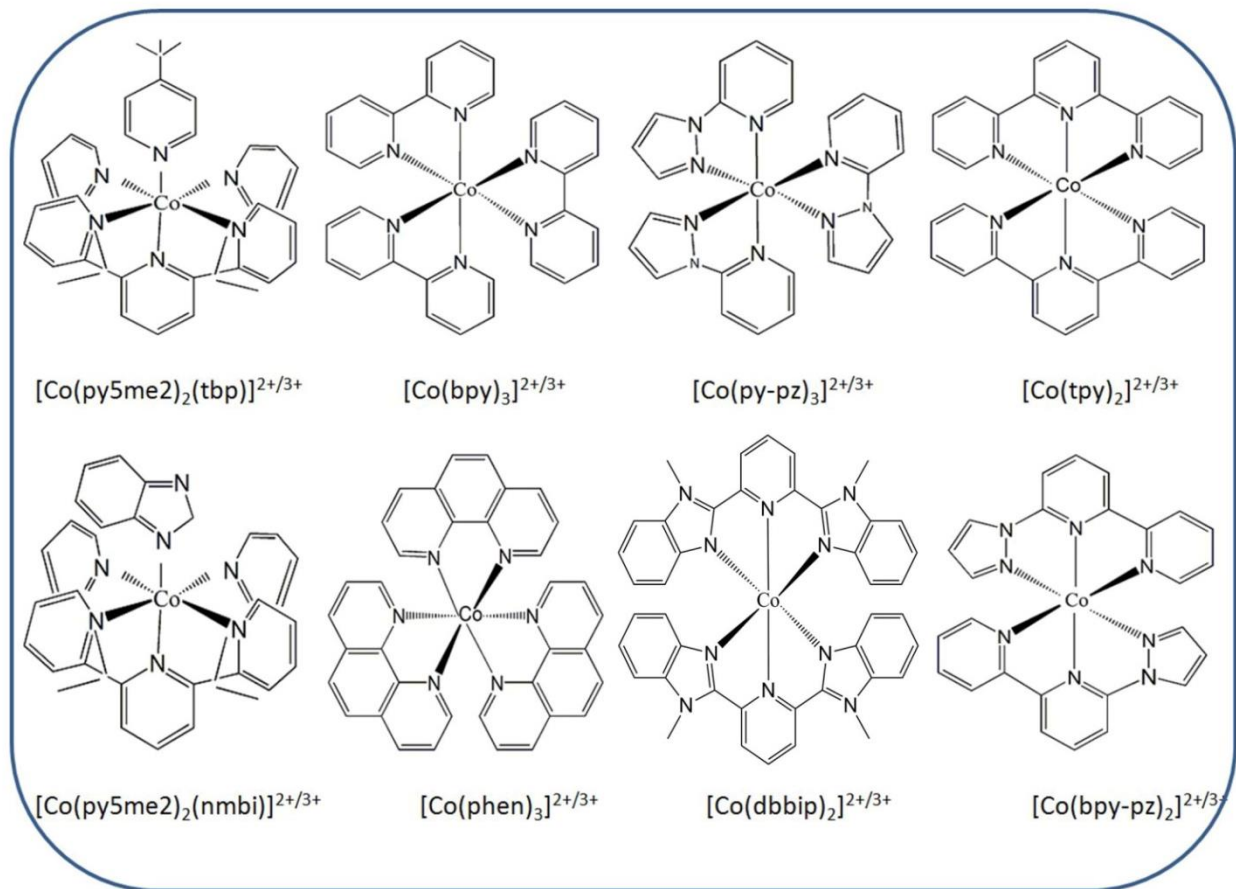


Fig. 2

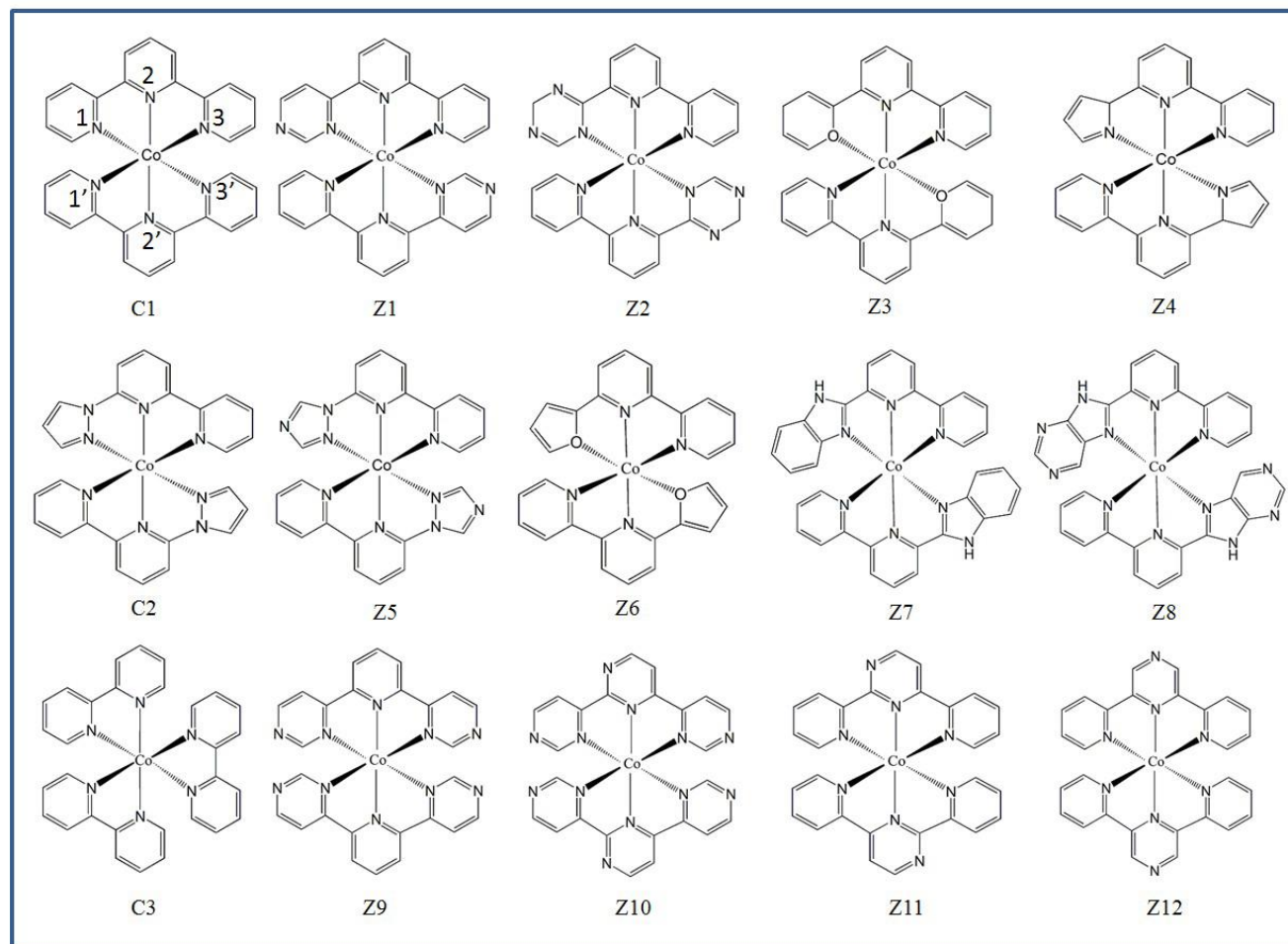


Fig. 3

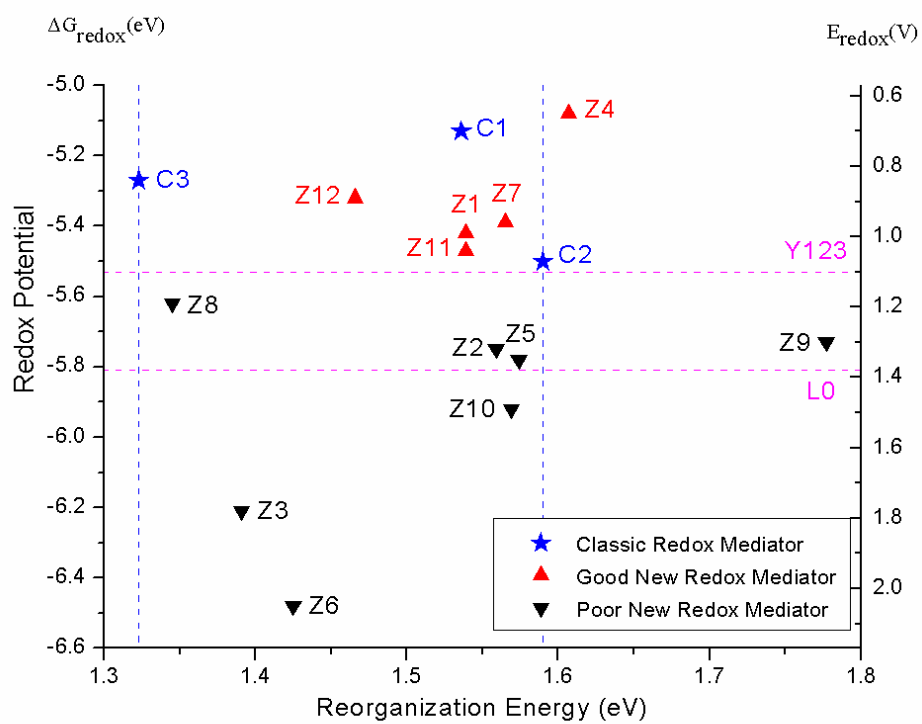


Fig. 4